Scaled model guidelines for formation flying solar coronagraph missions

FEDERICO LANDINI[1,*], MARCO ROMOLI[2], CRISTIAN BACCANI[2], MAURO FOCARDI[1], MAURIZIO PANCRAZZI[1], DAMIEN GALANO[3], AND VOLKER KIRSCHNER[3]

[1] INAF - Osservatorio Astrofisico di Arcetri, Largo E. Fermi 5, 50125 Firenze, Italy
[2] Università degli Studi di Firenze - Dipartimento di Fisica e Astronomia, Via Sansone 1, 50019 Sesto Fiorentino (Firenze), Italy
[3] ESA/ESTEC - Keplerlaan 1, NL-2200 AG Noordwijk ZH, The Netherlands
[*] Corresponding author: flandini@arcetri.astro.it

Compiled November 16, 2015

Stray light suppression is the main concern in designing a solar coronagraph. The main contribution to the stray light for an externally occulted space-borne solar coronagraph is the light diffracted by the occulter and scattered by the optics. It is mandatory to carefully evaluate the diffraction generated by external occulters and evaluate the impact that it has on the stray light signal on the focal plane. The scientific need for observations to cover a large portion of the heliosphere with an inner field of view as close as possible to the photospheric limb supports the ambition of launching formation flying giant solar coronagraphs. Their dimension prevents the possibility of replicating the flight geometry in a clean laboratory environment and the strong need for scaled model is thus envisaged. The problem of scaling a coronagraph has already been faced for exoplanets, for a single point source on axis at infinity. We face the problem here by adopting an original approach and by introducing the scaling of the solar disk as an extended source. © 2015 Optical Society of America

OCIS codes: *(260.1960) Diffraction theory; (350.1260) Astronomical optics; (220.4830) Systems design.*

http://dx.doi.org/10.1364/ao.XX.XXXXXX

1. INTRODUCTION

Historically, space-borne solar coronagraphs suffer from the high stray light level that prevents observations of the inner corona (below 1.3 solar radii, being the solar radius $R_\odot \simeq 7 \times 10^8$ m). In fact, the contrast between the inner corona and the solar photosphere in the visible is more than 6 orders of magnitude[1]; the visible-light corona is an optically thin medium, thus it is observable only out of the solar disk limb by occulting the photosphere with a suitable stop, and the stray light produced by the light diffracted by the occulter and scattered by the telescope optics dominates over the coronal signal at low heliocentric heights.
Usually, the inner corona is observable with the so-called internally occulted coronagraphs, that are characterized by a stop in the focal plane of the primary objective; the high level of stray light produced by the primary objective, that is directly hit by the photospheric light, prevent such a type of coronagraph from observing the extended corona (above 1.3 $R_\odot$). Externally occulted coronagraphs are more effective in reducing the stray light because the stop is placed in front of the primary objective. The main stray light source is in this case the light diffracted by the occulter and scattered by the optics. Externally occulted coronagraph are limited by vignetting problems at observing low in corona. Formation flight, the next frontier of visible-light space-borne externally occulted solar coronagraph, is thought in order to overcome this limitation. The larger the distance between the telescope entrance aperture and the occulter, the lower the level of stray light generated by the occulter inside the telescope pupil at fixed minimum field of view. Formation flying coronagraph are based on the principle of greatly increasing the distance between the occulter and the rest of the telescope, by using two different spacecrafts. PROBA-3ASPIICS [2, 3] (Association of Spacecrafts for Polarimetric and Imaging Investigation of the Corona of the Sun) and HiRISE [4] (High Resolution Imaging and Spectroscopy Explorer) are two examples. ASPIICS is currently approved by ESA in phase C/D and is characterized by an inter-satellite distance of $\sim$ 150 m and an occulter diameter of $\sim$ 1.5 m; its entrance aperture is 5 cm diameter wide and the telescope is based on the classical Lyot[5] and Evans[6] principles. HiRISE has been proposed for the next decade missions and it is huger than ASPIICS: the inter-satellite distance is 375 m and the occulter diameter is scaled accordingly.
The stray light management is the main driver for a solar coronagraph designer: all the necessary steps shall be taken in order to reduce the stray light as much as possible, while the residuals

shall be carefully evaluated and their impact on the expected coronal detection estimated.
Stray light measurements are not feasible with the 1:1 geometry: such tests are highly demanding in terms of environmental cleanliness (at least an ISO 5 clean room shall be used [7]) and it is not reasonable to build and maintain a dedicated large superclean facility for just an instrument.
A scaled model approach is therefore mandatory in order to evaluate the expected diffraction behind a giant coronagraph occulter.
The problem is being faced in exoplanet detection with stellar coronagraphs. They usually foresee distances of thousands of kilometers between the occulter and the telescope(e.g., [8]), and are therefore in the same conditions of impossibility to replicate the flight geometry in laboratory. The scaled model is designed by imposing that the same fresnel number (defined as the number of Fresnel zones that may be drawn within the aperture from a point on the image plane[9]) is obtained for the flight model and the mock-up geometrical configurations[10]. In solar coronagraphy with formation flying instruments, there is the additional complication of the extended source: the Sun cannot be considered as a point source at infinity (like the remote star for exoplanet coronagraphy) and its impact on the definition of the scaled model must be taken into account.
This paper is dedicated to the description of the guidelines that shall be adopted to design a scaled model of a solar coronagraph: section 2 shows the derivation of the scale law in the simple case of the point source at infinity, by using a different theoretical approach with respect to the one adopted in exoplanet coronagraphy. Solar coronagraphs external occulters are usually optimized by variously extending their shape along the optical axis: this aspect of the scaled model is discussed in section 3. Section 4 shows the law extension if the whole Sun is considered as a source.

2. SCALED MODEL FOR A POINT SOURCE AT INFINITY

We use figure 1 as a reference. According to the Fresnel-Kirchhoff

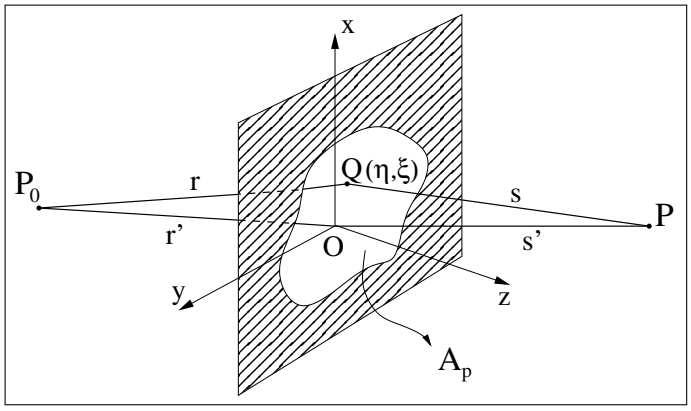


Fig. 1. Geometry for the definition of the Fresnel-Kirchhoff diffraction integral[11].

diffraction theory, the electromagnetic field U(P) given by the superposition of the wavelets generated by each point of an aperture, illuminated by a point source P_0, can be written as[11]:

$$U(P) = -\frac{Ai\cos(\delta)}{\lambda}\cdot \cdot \frac{\exp[ik(r'+s')]}{r's'}\iint_{A_p}\exp[ik\,f(\xi,\eta)]d\xi d\eta, \quad (1)$$

where $U(P)$ is the electromagnetic field in the image point P, A is a constant, i is the imaginary unit, k is the wave number, λ is the wavelength, δ is the angle between the line P_0P and the normal to the aperture plane; r is the distance from a point $Q(\xi,\eta)$ on the aperture A_p and P_0 (see figure 1), s is the distance between Q and P, r' and s' are the distances between P_0 and P and the origin of the frame of reference on the aperture plane, respectively. $dS = d\xi d\eta$ is the surface element on the aperture. $f(\xi,\eta)$ is the difference $(r+s)-(r'+s')$ expanded as a power series of ξ and η up to the second order:

$$f(\xi,\eta) = -\frac{x_0\xi+y_0\eta}{r'} - \frac{x\xi+y\eta}{s'} + \left[\frac{\xi^2+\eta^2}{2r'} + \frac{\xi^2+\eta^2}{2s'} + -\frac{(x_0\xi+y0\eta)^2}{2r'^3} - \frac{(x\xi+y\eta)^2}{2s'^3}\right]... \quad (2)$$

Let's consider the case of a circular aperture and a system that has circular symmetry. By assuming $r' \to \infty$, by setting the origin of the frame of reference at the intersection of the P_0P direction with the aperture plane, and by neglecting the higher order terms $\frac{(x_0\xi+y0\eta)^2}{2r'^3}$, $\frac{(x\xi+y\eta)^2}{2s'^3}$ we get:

$$U(P) = U(x) = -\frac{Ai}{\lambda}\frac{\exp[ikz]}{z}\iint_{A_p}\exp\left[ik\frac{\xi^2+\eta^2}{2z}\right]d\xi d\eta \quad (3)$$

where $s' = z$ is the distance between the occulter and the image plane (i.e., the plane where the diffraction is calculated) and x is the coordinate of the image point P. The limits of integration are defined according to the geometry of figure 2, where R_{EO} is the radius of the circular aperture.
The integral becomes:

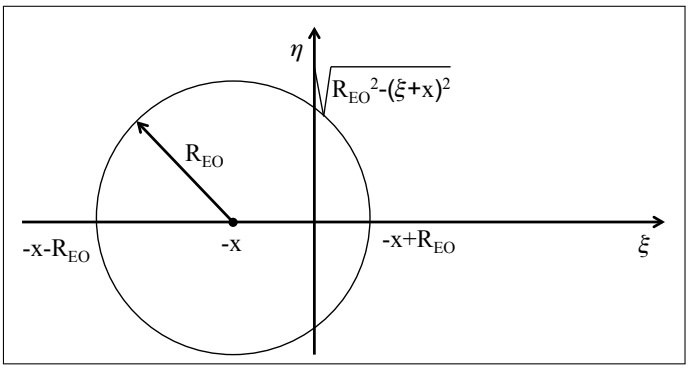


Fig. 2. Geometry for the definition of the extremes of the integral (3).

$$U(x) = -\frac{2Ai}{\lambda}\frac{\exp[ikz]}{z}\cdot \cdot \int_{-x-R_{EO}}^{-x+R_{EO}} d\xi \int_0^{\sqrt{R_{EO}^2-(\xi+x)^2}} \exp\left[ik\frac{\xi^2+\eta^2}{2z}\right]d\eta \quad (4)$$

In order to express the integral with adimentional quantities, we make the following substitutions:

$$\Xi = \frac{\xi}{R_{EO}},\ H = \frac{\eta}{R_{EO}},\ \Lambda = \frac{\lambda}{\lambda_0},\ Z = \frac{z}{z_0},\ X = \frac{x}{x_0} \quad (5)$$

where λ_0, z_0 and x_0 are the geometrical parameters of the scaled model, in the same units of λ, z and x, respectively.
The integral becomes:

$$U(X) = -\frac{2Ai}{\Lambda\lambda_0}\frac{\exp[ikZz_0]}{Zz_0}R_{EO}^2 \cdot \int_{-\frac{x_{x_0}}{R_{EO}}-1}^{-\frac{x_{x_0}}{R_{EO}}+1} d\Xi \int_0^{\sqrt{1-\left(\Xi+\frac{x_{x_0}}{R_{EO}}\right)^2}} \exp\left[i\frac{2\pi}{\Lambda\lambda_0}R_{EO}^2\frac{\Xi^2+H^2}{2Zz_0}\right] dH \quad (6)$$

In order to get $I_{APS}(x) = |U(x)|^2 = |U(\Xi)|^2$ (see equations (4) and (6)), that means invariant intensity of the diffracted light on the image plane, it must be:

$$\begin{cases} \frac{R_{EO}^2}{\lambda_0 z_0} = C' \\ \frac{x_0}{R_{EO}} = C'' \end{cases} \quad (7)$$

where C' and C'' are constants.
According to the Babinet principle, the light diffracted from an external occulter (EO) can be obtained by 1 minus the diffraction from an aperture with the same dimension of the occulter [12]. In the following part, we call I_{PS} the intensity of the diffraction produced by an external occulter of radius R_{EO}; it is defined similarly to the above defined I_{APS}.
It follows that in order to have the same diffraction intensity pattern I_{PS} in the flight model of the externally occulted coronagraph and in the laboratory scaled prototype, the same set of equations (7) is valid.
The first of equations (7) shows that in order to scale the EO dimension by a factor f, λ and z shall be scaled by the same factor. In laboratory, a change to the wavelength can be really challenging. For example, if the coronagraph is working in the visible, a scale factor f =10 would push down the scaled wavelength to the EUV, that is not easily achievable, even in the hypothesis that the laboratory facility is designed to work in the vacuum regime. In order to keep the wavelength unscaled, the distance between the occulter and the image plane shall be scaled by a factor f^2. The scheme, in the case of a point source at infinity, is pictorially summarized in figure 3 (a).
The second of equations (7) means that a factor f applied to the EO dimension shall be linearly adopted for the image plane sampling as well.
The obtained result is the same that is found for exoplanetary coronagraphy [10], which at any rate does not take into account the extension of the source, being the source in such cases a single point on axis at infinity.

3. OPTIMIZED OCCULTERS

In order to suppress the level of diffracted light behind the EO, solar coronagraphs need to implement occulters with an optimized geometry.
Newkirk and Eddy [13], during a balloon flight, proved that not-optimized occulters fail in fulfilling their goal, since the light diffracted by the occulter edge and scattered by the telescope optics overwhelms the coronal signal. A long debate [14–19] is ongoing in the solar community on the best optimizing shape, and the answer is not univocal. The optimization technique shall be adapted to the mission requirements and to the coronagraph

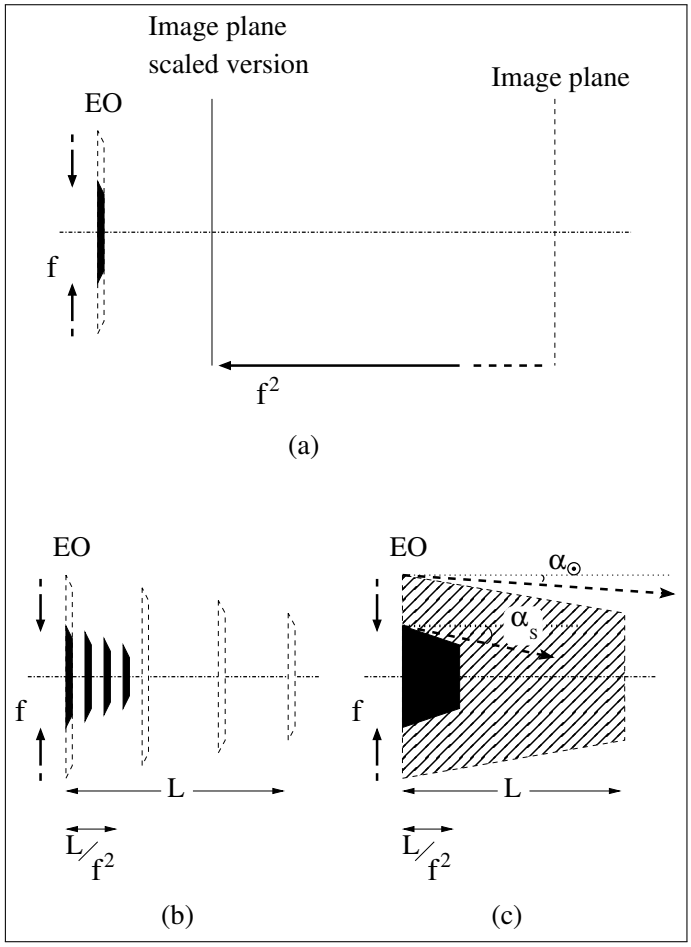


Fig. 3. Scale law for a point source at infinity. Dashed line: not-scaled geometry. Solid line: scaled geometry. (a) Summary of the scale law for a point source at infinity. (b) Adopted scheme to scale longitudinally a multiple disks system. (c) Adopted scheme to scale a frustum of a right cone.

performance goals. Up to now, serrated edges, multiple disks systems and a multithreaded frustum of a right cone have been used.The majority of flown solar coronagraphs in the visible adopted a multiple disk system as an external occulter. This introduces the issue of scaling an occulter that has an optically functional shape along the optical axis. In other words, how to scale longitudinally the occulter?
An external occulter optimized by a solid shape along the optical axis (like, for instance, a frustum of a right cone) can be thought as the logical improvement of the multiple disks system, with an infinite number of disks over a finite longitudinal length. Thus, in principle, the scale law for a multiple disks system can be extended to a solid longitudinal shape.
Figures 3 (b) and (c) explicit the logical extension from the multiple disks case to the solid case.
In the case of a multiple disks system, the diffraction behind the occulter can be calculated in multiple serial steps. First, the diffraction as generated by the outer disk (i.e., that facing the source) is calculated on the plane of the second disk. Then, the diffraction as generated by the second disk is calculated on the plane of the third disk. And so on, recursively, until the plane of the last disk. The electromagnetic field amplitude and phase, as evaluated on each point of the plane of the last disk, generate

the final diffraction pattern on the image plane. In order to have the same diffraction pattern on the image plane in the real model and in the scaled model, the diffraction patterns evaluated for the real and the scaled configurations must overlap for each disk plane. So, as shown in figures 3 (b) and (c), the longitudinal scale factor f^2 shall be applied either to the length L of the spindle that supports the disks (figure 3 (b)) and to the length of the solid occulter (figure 3 (c)).

4. THE WHOLE SUN AS A SOURCE

In order to take into account the whole solar disk as a source, a convolution is performed of the plane wave diffraction pattern intensity I_{PS} with a kernel sized as the solar disk as projected on the entrance aperture plane.
The convolution integral is given by:

$$I(r,\theta) = \int_0^{2\pi} d\hat{\theta} \int_0^{\infty} I_{PS}(r-\rho, \hat{\theta}-\theta) \cdot Disk(\rho,\theta)\rho d\rho \quad \textbf{(8)}$$

where $Disk(\rho,\theta)$ is the function that defines the irradiance of the solar disk. It is actually not dependent on θ and can be defined as:

$$Disk(\rho) = \begin{cases} \mathcal{L}(\rho) & \text{if } \rho \leq R'_{\odot} \\ 0 & \text{if } \rho > R'_{\odot} \end{cases} \quad \textbf{(9)}$$

where $\mathcal{L}(\rho)$ is a limb darkening model, which is wavelength dependent, and $R'_{\odot} = z \cdot \tan(\alpha_{\odot})$ is the projection of the solar disk radius on the image plane. $\alpha_{\odot}$is the semi-divergence of the solar disk.
With this information, equation (8) may be rewritten as:

$$I(r) = 2\pi \int_0^{R'_{\odot}} I_{PS}(r-\rho) \cdot \mathcal{L}(\rho)\rho d\rho \quad \textbf{(10)}$$

where the dependence on θ has been dropped according to the symmetry of the system. We adopt the same approach of section 2 by normalizing the variables in order to work with adimensional quantities:

$$P = \frac{\rho}{x_0}, \; R = \frac{r}{x_0} \quad \textbf{(11)}$$

The integral becomes:

$$I(R) = 2\pi \int_0^{R'_{\odot}/x_0} I_{PS}\left(x_0(R-P)\right) \cdot \mathcal{L}(P)\, x_0^2\, P\, dP \quad \textbf{(12)}$$

In order to have $I(R,\theta) = I(r,\theta)$ it must be:

$$\frac{R'_{\odot}}{x_0} = C''' \quad \textbf{(13)}$$

where C''' is a constant. This means that even the dimension of the projection of the solar disk on the pupil plane has to be scaled by the same factor f that is used to scale the occulter dimension.
It is interesting to understand which is the significance of this conclusion on the scaled laboratory set-up. Usually, the stray light suppression performance of classic solar coronagraphs (i.e., not formation flying ones) is performed in a clean room environment, in front of a solar simulator. A solar simulator is a source that replicates the solar divergence at a given heliocentric distance over a certain wavelength band.
In the scaled model case, the simulated Sun has to vary according to the desired size of the projection of the solar disk on the image plane. In order to retrieve the relationship between the scaled simulated Sun divergence, α_S, and the real one, $\alpha_{\odot}$, we solve the following simple linear system of equations:

$$\begin{cases} R'_S = \dfrac{R'_{\odot}}{f} \\ R'_{\odot} = z \cdot \tan(\alpha_{\odot}) \\ R'_S = \dfrac{z}{f^2} \cdot \tan(\alpha_S) \end{cases} \quad \textbf{(14)}$$

where for the first equation the scale law defined by (13) has been used. The relationship between α_S and $\alpha_{\odot}$ is thus given by:

$$\tan(\alpha_S) = f \cdot \tan(\alpha_{\odot}) \quad \textbf{(15)}$$

which implies that the scaled simulated solar divergence shall be increased by the same factor f that is used to decrease the EO dimension.
The definition of the half-aperture angle of a conical occulter is linked to the geometry of the coronagraph and to the solar disk divergence. In fact, the conical surface shall be in the shadow of the front face of the cone (the one that faces the solar disk) with respect to the solar disk. Figure 3 (c) emphasizes how, by following the scale law, the truncated cone aperture is harmonized with the increased divergence of the scaled solar disk.

5. CONCLUSIONS

We presented a discussion about the guidelines to be adopted to design a scaled model of an externally occulted space-borne solar coronagraph. The aim is to help in designing scaled laboratory prototypes to be used to measure the diffraction generated by the external occulter on the telescope entrance aperture plane.
The argument has been recently faced for exoplanets coronagraphs with a method based on the invariance of the Fresnel zones configuration out of the occulter edge. We adopt here an original point of view based on the Fresnel-Kirchhoff diffraction integral and we broaden the problem to the case of an extended source for the diffraction evaluation. In fact, the solar disk cannot be considered as a point source at infinity and can be thought as an infinite set of incoherent point sources over a finite bi-dimensional surface.
The scale law we define is the same that is found for exoplanetary coronagraphy for a single point source on axis at infinity: if the occulter dimension is scaled by a factor f, the distance between the occulter and the entrance aperture shall be scaled by a factor f^2. As for the extended source case, a laboratory solar simulator shall be able to generate a solar divergence that is increased by a factor f, which is not trivial. In most cases, a trade-off will be necessary between the dimension of the scaled coronagraph and the divergence of the simulated Sun.

REFERENCES

1. A. N. Cox, *Allen's Astrophysical Quantities* (AIP press, Springer-Verlag, New York, 2000).
2. S. Vives *et al.*, "Formation flyers applied to solar coronal observations: the ASPICS mission," (2005), vol. 5901 of *Proc. SPIE*, pp. 590116.1–11.
3. P. Lamy and L. Damé, "ASPIICS: a giant coronagraph for the ESA/PROBA-3 Formation Flying Mission," in "Space Telescopes and Instrumentation 2010: Optical, Infrared, and Millimeter Wave," , vol. 7731 of *Proc. SPIE* (2010), vol. 7731 of *Proc. SPIE*, pp. 773118.1–12.

4. L. Damé, "Future solar space missions to observe the Sun from the chromosphere to the corona and beyond," Proceeding of the 2nd symposium IAGA (2010).
5. B. Lyot, "Étude de la couronne solaire en dehors des éclipses. Avec 16 figures dans le texte." Zeitschrift fur Astrophysics **5**, 73 (1932).
6. J. W. Evans, "Photometer for measurement of sky brightness near the sun," J. Opt. Soc. Am. **38**, 1083 (1948).
7. Y. Stockman *et al.*, "Conceptual design of a stray light facility for earth observation satellites," (2012), Proceedings of the ICSO.
8. N. J. Kasdin *et al.*, "Using starshades to image exoplanets," SPIE Newsroom (2013).
9. e. i. c. M. Bass, *Handbook of optics - Vol I* (McGraw-Hill, USA, 1995).
10. D. Sirbu *et al.*, "Scaling relation for occulter manufacturing errors," in "Techniques and Instrumentation for Detection of Exoplanets VII," , vol. 9605 of *Proc. SPIE* (2015), vol. 9605 of *Proc. SPIE*, pp. 96052E–1–12.
11. M. Born and E. Wolf, *Principles of Optics* (Cambridge University Press, Cambridge, 2001).
12. C. Aime, "Theoretical performance of solar coronagraphs using sharp-edged or apodized circular external occulters," A&A **558**, A138.1–10 (2013).
13. G. Newkirk, Jr. and J. A. Eddy, "A Coronograph Above the Atmosphere," S&T **24**, 77 (1962).
14. G. Newkirk, Jr. and D. Bohlin, "Reduction of scattered light in the coronagraph," App. Opt. **2**, 131–140 (1963).
15. B. Fort *et al.*, "The reduction of scattered light in an external occulting disk coronagraph," A&A **63**, 243–246 (1978).
16. A. V. Lenskii, "Theoretical evaluation of the efficiency of external occulting systems for coronagraphs," Sov. Astron. **25**, 366–372 (1981).
17. S. Koutchmy, "Space born coronagraphy," Sp. Sc. Rev. **47**, 95–143 (1988).
18. M. Bout *et al.*, "Experimental study of external occulters for the Large Angle and Spectrometric Coronagraph 2: LASCO-C2," App. Opt. **39**, 3955–3962 (2000).
19. F. Landini *et al.*, "External occulter laboratory demonstrator for the forthcoming formation flying coronagraphs," App. Opt. **50**, 6632–6644 (2011).